

# X-Ray crystallographic studies of recombinant inorganic pyrophosphatase from *Escherichia coli*

V.Yu. Oganessyan<sup>a</sup>, S.A. Kurilova<sup>b</sup>, N.N. Vorobyeva<sup>c</sup>, T.I. Nazarova<sup>b</sup>, A.N. Popov<sup>a</sup>,  
A.A. Lebedev<sup>a</sup>, S.M. Awaeva<sup>b</sup>, E.H. Harutyunyan<sup>a,\*</sup>

<sup>a</sup>Institute of Crystallography, Russian Academy of Sciences, Leninsky pr. 59, Moscow 117333, Russian Federation

<sup>b</sup>A.N. Belozersky Institute of Physico-Chemical Biology and <sup>c</sup>Chemical Department, Moscow State University, Moscow, Russian Federation

Received 23 May 1994

## Abstract

An *E. coli* inorganic pyrophosphatase overproducer and a method for a large-scale production of the homogeneous enzyme are described. The inorganic pyrophosphatase was crystallized in the form containing one subunit of a homohexameric molecule per asymmetric unit: space group R32,  $a = 110.4$  Å,  $c = 76.8$  Å. The electron density map to 2.5 Å resolution phased with Eu- and Hg-derivatives (figure of merit,  $\langle m \rangle = 0.51$ ) was improved by the solvent flattening procedure ( $\langle m \rangle = 0.77$ ). The course of the polypeptide chain and the secondary structure elements, intersubunit contacts and positions of the active sites were characterized. Homology with *S. cerevisiae* inorganic pyrophosphatase structure was found.

**Key words:** *E. coli* inorganic pyrophosphatase; X-ray structure; Recombinant vector; Expression

## 1. Introduction

Inorganic pyrophosphatase (EC 3.6.1.1) (PPase) hydrolyzes inorganic pyrophosphate in the cell. An X-ray investigation to 3.0 Å resolution has only been carried out for the dimer molecule of *Saccharomyces cerevisiae* PPase [1]. An understanding of the chemical mechanism of the substrate conversion is hindered by the absence of data on the three-dimensional structure of the native protein, its complexes, and mutants.

This work presents a basic stage of the X-ray structure analysis of hexamer molecule of *E. coli* PPase. It includes the construction of an overproducer, the large-scale production of the homogeneous enzyme and its crystallization, the obtaining of the heavy-atom derivatives, and X-ray analysis at 2.5 Å resolution. This is the first three-dimensional structure of a prokaryotic pyrophosphatase to be described.

## 2. Experimental

### 2.1. Crystallization

*E. coli* inorganic pyrophosphatase was crystallized by a slightly modified technique described in [2]. Crystals of maximum size  $0.6 \times 0.6 \times 0.5$  mm<sup>3</sup> were grown for 10–15 days. They belonged to space group R32, with unit cell dimensions  $a = 110.4$  Å,  $c = 76.8$  Å, and diffracted to 2.0 Å resolution. The asymmetric part of the unit cell contained one subunit of the hexamer.

### 2.2. Data collection and processing

X-ray data sets for the native enzyme and two derivatives (Eu and Hg) were measured on a KARD-4 automatic diffractometer with a two-dimensional detector designed at the Institute of Crystallography (Cu-K $\alpha$  irradiation, graphite monochromator). Each data set for crystals of the native protein and derivatives was obtained from one crystal. The X-ray data statistics are given in Table 1.

### 2.3. Structure determination

Structure calculations were carried out on a PC-386 with the Blanc program written by A.A. Vagin [3].

Interpretation of the data for the heavy atom derivatives showed the presence of one major binding site in each derivative. Calculations of difference syntheses using the final phases set did not reveal any minor sites of heavy atoms.

Electron density synthesis at 2.5 Å resolution for the phases obtained using two derivatives ( $\langle m \rangle = 0.51$ ) turned out to be uninterpretable. To improve the phases, the Wang procedure [4], utilizing solvent flattening, was used. Four cycles of phase calculations by this technique, combined with isomorphous phases, improved the value of  $\langle m \rangle$  to 0.77. The value of  $R = |F_{\text{obs}} - F_{\text{calc}}| / \langle F_{\text{obs}} \rangle$  dropped from 0.49 to 0.32, the value of correlation factor  $C(F_o, F_c) = \sum (F_o - \langle F_o \rangle)(F_c - \langle F_c \rangle) / (\sum (F_o - \langle F_o \rangle) \sum (F_c - \langle F_c \rangle))$  ( $F_o$  and  $F_c$  are the observed and calculated structure factor amplitudes, respectively) rose from 0.71 to 0.88.

The electron density distribution, contoured at the  $2\sigma$  level, showed gaps in several places. However, tracing of the polypeptide chain and localization of the major part of bulky amino acid residues using the known amino acid sequence [5] on this synthesis was unambiguous. The model building procedure on interactive graphic system Evans & Sutherland PS with the O program [6] was used to trace the polyaniline chain. At present the refinement of the protein atomic model at 2.2 Å resolution is being carried out ( $R = 30\%$ ).

### 2.4. Obtaining of a recombinant *E. coli* PPase

The polymerase chain reaction was used to amplify a DNA segment containing the *ppa* gene of the known sequence [5,7]. The 1.1 kb fragment was treated with *AccI* and *BglI* to produce a 0.8 kb fragment, containing the intact *E. coli ppa* gene and its regulatory elements. The blunt-ended *accI*–*BglI* fragment was ligated into the *SmaI* site of plasmid pUC19. The resulting recombinant plasmid was used for transformation of *E. coli* strain JM109.

The 75-fold amplification of the plasmid-encoded PPase, as compared with the chromosomal one, raised the PPase production to about 1.5% of the cell weight and to about 15% of the protein content.

\*Corresponding author. Fax: (7) (095) 135 1011.

Table 1  
X-ray data statistics

Derivative	$1/2\sin\theta$	$N$	$N_{\text{ind}}$	% $I > 3\sigma$	$R_{\text{sym}}$	$R_{\text{stand}}$
Native	2.19	26800	9116	87	6.3	5.05
Hg	2.30	22100	7253	81	8.3	10.3
Eu	2.50	18400	6169	92	8.0	7.0

$N$ , full number of measured reflections;  $N_{\text{ind}}$ , number of independent reflections;  $\sigma$ , root mean square deviation in intensity measurements;  $R_{\text{sym}} = \sum |<I> - I| / \sum <I>$ ;  $R_{\text{stand}} = \sum \sigma(I) / \sum I$ .

### 3. Results and discussion

#### 3.1. Structure description

Fig. 1 presents a schematic drawing of the *E. coli* inorganic PPase hexamer molecule structure. The molecule is centered at a special position of the unit cell with coordinates  $x = 0$ ,  $y = 0$ ,  $z = 1/2$ , where the three crystallographic two-fold axes and the three-fold axis perpendicular to them are intersecting. All the hexamer subunits are crystallographically identical.

The polypeptide chain course is shown in Fig. 2. The structure was found to have 3  $\alpha$ -helices and 9  $\beta$ -strands. From the N-terminus up to residue 86 the polypeptide chain forms mostly  $\beta$ -strands, while the elongated  $\alpha$ -helices are localized mainly in the C-terminal part. The distribution of amino acid residues among the secondary structure elements is given in Table 2. The non-regular fragments are rather long. The subunit core is formed by a 7-strand  $\beta$ -sheet which comprises, starting with the outer side of the molecule, the following  $\beta$ -strands:  $\beta 9$ ,  $\beta 7$ ,  $\beta 8$ ,  $\beta 5$ ,  $\beta 4$ ,  $\beta 1$  and  $\beta 6$ . Strands  $\beta 8$  and  $\beta 5$  are parallel to each other; the remaining pairs of  $\beta$ -strands are in an antiparallel position. This sheet might be arbitrarily sub-

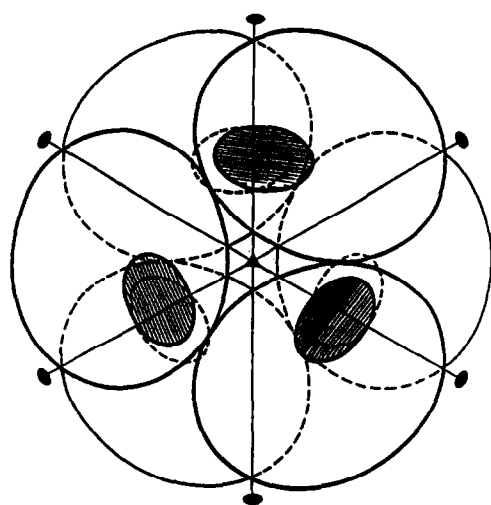


Fig. 1. A scheme of the quaternary structure of hexameric *E. coli* inorganic pyrophosphatase. Molecular diads (●) and a triad (▲) are shown. Small dashed regions indicate the positions of active sites in the upper trimer subunits. Those of the lower trimer are shown by dashed lines.

divided into two parts. The first, in the subunit inner part, comprises the last four  $\beta$ -strands, and the second comprising the first three  $\beta$ -strands. Four  $\beta$ -strands, together with the double ribbon, the non-regular fragment 59–64 preceding the  $\beta 5$  strand, and the elongated  $\beta 4$  fragment can be assigned to an independent  $\beta$ -type domain. The three central sheet  $\beta$ -strands, the  $\alpha 2$  and  $\alpha 3$  helices covering them, and the preceding fragment 109–122, including the  $\alpha 1$  helix, can be assigned to the second domain, a mixed  $\alpha/\beta$ -type.

The spatial division of the domains along the polypeptide chain course is most clearly observed in the active site formation region (Fig. 2B). Joining of the two domains gives rise to a barrel structure. It includes five  $\beta$ -strand fragments: 104–107, 67–72, 55–58 and 16–18.

#### 3.2. Comparison of the PPase structures

Currently, the primary structure of eight PPases is known. Despite the low homology between them, a remarkable conservation of 24 residues was demonstrated [8]. Part of them are essential for the secondary structure formation, and the remainder are directed towards the active site cavity [1]. A comparison of the polypeptide chain course in *S. cerevisiae* and *E. coli* PPases (comprising 286 and 175 amino acid residues, respectively) showed that both structures are spatially homologous (Fig. 3). The mutual position of the central  $\beta$ -sheet, barrel structure,  $\alpha$ -helices and most of the  $\beta$ -strands is similar in both structures.

#### 3.3. Intersubunit contacts

The intersubunit contact sites in the hexamer molecule can be readily analyzed from Fig. 4. The system of amino acid contacts in the first two subunits may turn out to be rather evolved. The double ribbon of one subunit, including more than 20 amino acid residues, is drawn

Table 2  
Distribution of amino acid residues among secondary structure elements

$\beta 1$	12–22	$\beta 2$	27–34	$\beta 3$	39–45
$\beta 4$	52–58	$\beta 5$	67–74	$\beta 6$	79–86
$\beta 7$	87–96	$\beta 8$	101–107	$\beta 9$	147–156
$\alpha 1$	111–118	$\alpha 2$	126–146	$\alpha 3$	157–173

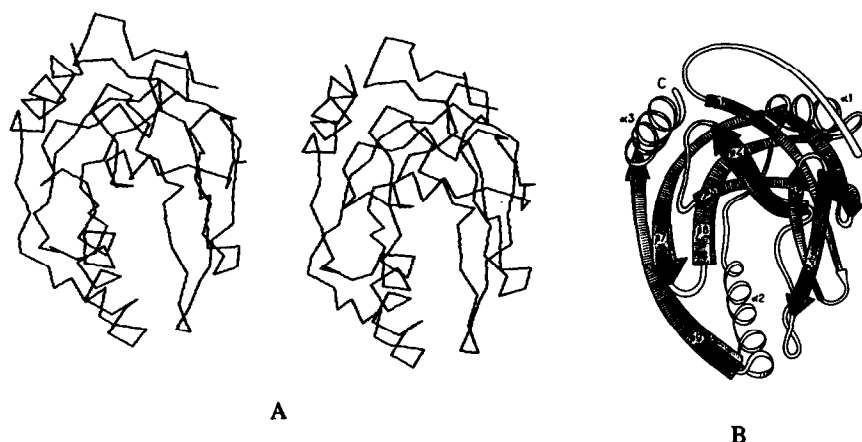


Fig. 2. Stereo (A) and artistic (B) drawings of the polypeptide chain backbone in the *E. coli* PPase subunit. Helices (spirals),  $\beta$ -strands (rods), and irregular segments (double thin lines) are shown.

close to all secondary structure elements of the second subunit that form the outer part of the barrel structure. As the ribbon top is also close to the N-terminus of the subunits, this may give rise to another contact site engaging all three subunits of the trimer.

The contact site between the top and bottom left subunits is made up by polypeptide chain fragments involved in the active site formation. The most evolved system of contacts appears between the two parallel  $\alpha 2$  helices which run close together, and 46–50 fragments of these subunits. So the active sites of these two subunits are the most closely drawn together.

The polypeptide chains of the two subunits related by another symmetry double axis are removed further than in other contact regions described above. However, interaction between side groups of the N-terminal fragments of  $\alpha 1$  and  $\alpha 2$  helices must not be ruled out.

### 3.4. Active site

The polypeptide chain of inorganic pyrophosphatase

forms several cavities. One of them arises between the two domains.

The left wall of this cavity is formed by the following fragments of the central sheet  $\beta$ -strands: 98–104, 147–149, and the  $\alpha$ -helix C-terminal fragment 132–140. Side groups of the C-terminal fragments of the  $\alpha$ -helix, together with those of  $\beta 4$ , form the bottom of the active site cavity. The right wall is made up of two elongated embedded loops 37–48 and 21–37, two close branches of which are combined into a double curved ribbon. The top of the active site cavity is made up by fragments 50–54 and 65–70. The above-listed polypeptide chain fragments forming the active site cavity include all the conserved amino acid residues, which, as can be seen from the data on the *S. cerevisiae* PPase spatial structure, are evidently essential for enzyme activity.

The results of the present work offer the promise of successful X-ray analysis of *E. coli* PPase complexes with metal-activators, metal-activators and phosphate, and metal-activators and substrate analogs. The three-dimensional structure of *E. coli* PPase mutants will be investigated, too.

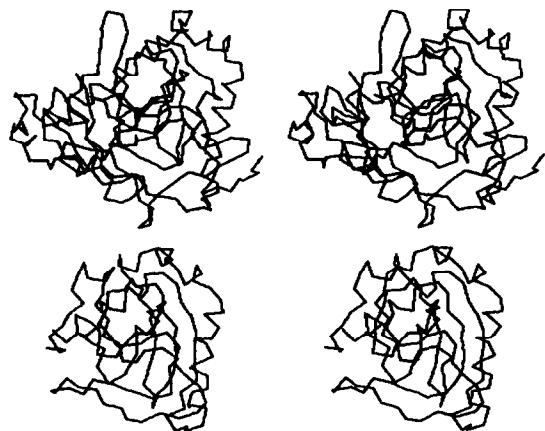


Fig. 3. A stereo drawing of the course of the polypeptide chain in the *E. coli* (lower panel) and *S. cerevisiae* (upper panel) PPase subunit.

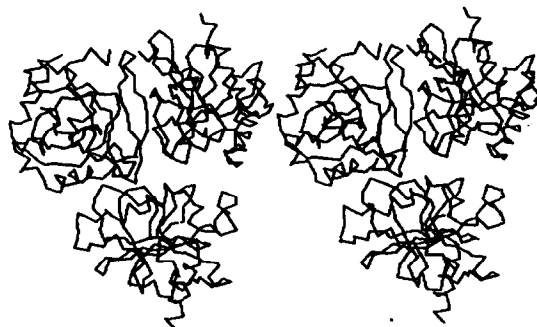


Fig. 4. A stereo drawing of contacting *E. coli* subunits. Two upper subunits are related by a molecular 3-fold axis. They are related to the lower subunit by molecular two-fold axes.

**Acknowledgements:** This work was financed by the Russian Foundation for Basic Research and the International Science Foundation. The authors are grateful to M.N. Isupov for his valuable advice on calculation techniques, to Dr. T.S. Oretskaya who prepared the oligonucleotides, and to I.L. Tolstova for assistance in writing this paper.

## References

- [1] Terzyan, S.S., Voronova, A.A., Smirnova, E.A., Kuranova, I.P., Nekrasov, Yu.V., Arutyunyan, E.G., Vainshtein, B.K., Hohne, W. and Hansen, G. (1984) *Bioorg. Khim.* 10, 1469–1482.
- [2] Airumyan, L.G., Nazarova, T.I., Kurilova, S.A. and Avaeva, S.M. (1990) *Vestnik Moscovskogo Universiteta, Serya khimiya* 31, 98–100.
- [3] Vagin, A.A. (1983) Candidate thesis in physics and mathematics, Institute of Crystallography of Russian Academy of Sciences, Moscow.
- [4] Wang, B.C. (1985) *Methods Enzymol.* 15, 90–112.
- [5] Lahti, R., Pitkaranta, T., Valvbe, E., Ilta, I., Kukko-Ralske, E. and Heinonen, J. (1988) *J. Bacteriol.* 170, 5901–5907.
- [6] Jones, T.A., Zou, S.-Y., Cowan, S.W. and Kjeldgaard, M. (1991) *Acta Cryst.* A47, 110–119.
- [7] Sambrook, J., Fritsch, E.F. and Maniatis, T. (1989) in: *Molecular Cloning: A Laboratory Manual*, Cold Spring Harbor Laboratory Press, NY, pp. 21–104.
- [8] Cooperman, B.S., Baykov, A.A. and Lahti, R. (1992) *Trends Biochem. Sci.* 17, 262–266.